LBL-33969
UC-210
Preprint

Lawrence Berkeley Laboratory
UNIVERSITY OF CALIFORNIA

Materials Sciences Division

Submitted to Journal of the Electrochemical Society

Rechargeable Na/Na_xCoO_2 and $Na_{15}Ph_4/Na_xCoO_2$ Polymer Electrolyte Cells

Y. Ma, M.M. Doeff, S.J. Visco, and L.C. De Jonghe

April 1993

Prepared for the U.S. Department of Energy under Contract Number DE-AC03-76SF00098

DISCLAIMER

LBL-33969
UC-210

Rechargeable Na/Na_xCoO_2 and $Na_{15}Pb_4/Na_xCoO_2$ Polymer Electrolyte Cells

Yanping Ma, Marca M. Doeff, Steven J. Visco

and Lutgard C. De Jonghe

Materials Sciences Division

Lawrence Berkeley Laboratory

University of California

Berkeley, CA 94720

April 1993

This work was supported by the Assistant Secretary for Conservation and Renewable Energy, Office of Transportation Technologies, Electric & Hybrid Propulsion Division of the U.S. Department of Energy under Contract No. DE-AC03-76SF00098.

Abstract

Cells using polyethylene oxide as a sodium ion conducting electrolyte, P2 phase Na_xCoO_2 as the positive and either sodium or sodium/lead alloy as the negative were assembled, discharged and cycled. Na_xCoO_2 intercalates sodium over a range of x = 0.3-0.9, giving theoretical energy densities of 1600 Wh/L (for sodium) or 1470 Wh/L (for sodium/lead alloy). Cells could be discharged at rates up to 2.5 mA/cm^2 corresponding to 25% depth of discharge and were typically discharged and charged at 0.5 mA/cm^2 (100% depth of discharge) or approximately 1-2 C rate. Over one hundred cycles to 60% utilization or more, and two hundred shallower cycles at this rate have been obtained in this laboratory. Experimental evidence suggests that the cathode is the limiting factor in determining cycle life and not the Na/PEO interface as previously thought. Estimates of practical energy and power densities based upon the cell performance and the following configuration are presented: 30 to 45 w/o electroactive material in the positive electrode, a two-fold excess of sodium, 10 μm separators and 5 μm current collectors composed of metal coated plastic. On the basis of these calculations, practical power densities of 335 W/L for continuous discharge at 0.5 mA/cm^2 and up to 2.7 kW/L for short periods of time should be attainable. This level of performance approaches or exceeds that seen for some lithium/polymer systems under consideration for electric vehicle applications, but with a lower anticipated cost.

Introduction

Advanced battery systems combining an alkali metal, a solid polymer electrolyte (SPE) and an intercalation compound as cathode have recently been proposed for use in electric vehicle and other applications. The all solid state components allow flexibility of cell design, ease of stack assembly and improved safety characteristics, and the polymer electrolyte allows operation at moderate temperatures (from about 70 - 100° C). The vast majority of studies have been directed towards the very promising lithium systems, but recent results obtained on amorphous MoS_3[1], $Na_xCr_3O_8$[2] and vanadium oxides[3] prove that sodium cells can indeed function with solid polymer electrolytes. However, much improvement in energy density, rate capability and cyclability is required before sodium/SPE batteries can be considered for practical uses. Because of the lower capacity density and voltage (vs. SHE) compared to lithium, energy densities are expected to be lower for cells utilizing sodium. Additionally host materials commonly used as cathodes tend to intercalate sodium to a lesser extent than lithium due to the larger ionic radius, further reducing energy densities. Still, the much lower cost of sodium[4] compared to lithium makes development of Na/SPE systems a compelling goal (Table 1).

Clearly, the challenge is to find a cathode material that can intercalate sodium to a large extent and thus allows a high theoretical energy density in sodium batteries. Furthermore, the material should exhibit good reversibility and rate capability. Sodium cobalt bronzes have recently been shown to exhibit these characteristics as well as excellent performance in cells with liquid organic

electrolytes[5]. These compounds exist in several phases depending upon composition (x in Na_xCoO_2) and the method of preparation[6,7]. Most notably the P2 phase Na_xCoO_2 has been shown to undergo electrochemical intercalation and de-intercalation of sodium reversibly over a range of approximately x= 0.3 - 0.9 without structural changes. For the present study, the P2 sodium cobalt bronze was used as a cathode for cells with solid polymer electrolytes and sodium or sodium/lead alloy anodes. As will be shown, cells utilizing this material have exhibited the highest performance for a sodium/SPE system to date in terms of rate capability, cyclability and energy densities. Sodium/polymer batteries can, therefore, now be considered as practical alternatives for applications in which cost control as well as performance is critical, such as in electric vehicles.

Experimental

The sodium cobalt bronze $Na_{0.7}CoO_2$ was prepared in the P2 phase as described previously[5,6]. In brief, mixtures of Na_2O_2 and Co_3O_4 in the desired stoichiometric ratio were ground and well mixed, and then formed into pellets. The pellets were heated to 750° C under oxygen for thirty hours, and the resulting product ground into fine powders of less than 2 μm in diameter, as determined by scanning electron microscopy. The product was identified by X-ray diffraction. The density of $Na_{0.7}CoO_2$ was determined by Corning Incorporated, Corning N. Y..

Composite electrodes were made by casting mixtures of the electroactive material, carbon, polyethylene oxide (PEO), sodium trifluoromethanesulfonate (NaTf, in a ratio of eight ethylene oxide units per sodium) and a carbon dispersant

in acetonitrile onto Teflon coated glass plates. After air drying, the electrodes were cut to the desired size and dried in vacuum for seventy-two hours or longer. Polymer electrolytes of composition $P(EO)_8NaTf$ were made in a similar fashion.

Sodium from Alfa products was purified prior to use in cells in the following manner. The metal was melted, filtered through coarse stainless steel wool, and then heated to 400° with small amounts of titanium sponge. The purified sodium was rolled between sheets of polyethylene to form thin foil electrodes. $Na_{15}Pb_4$ alloy was made by melting sodium with lead and then purified as above. The alloy was heated in a stainless steel ring to form flat electrodes for use in cells.

Cathode-limited cells were assembled in a helium-filled glove box with O_2 levels below 1 ppm, and heated to 90° C (for sodium) or 100° C (for sodium/lead alloy) prior to use to render the polymer electrolytes conductive. Galvanostatic charges and discharges were performed at 0.1-3.0 mA/cm^2 using a computer controlled PAR 173 or 371 potentiostat/galvanostat and software developed in this laboratory. The current was interrupted periodically (for some experiments) to estimate cell open circuit voltages (OCVs).

A four-probe technique developed for solid polymer electrolyte cells[8] was used to evaluate the limitations of each component on performance. Sodium foils were used as internal reference electrodes, and cells were subjected to galvanostatic charges and discharges as well as to sequential bipolar square-wave current pulses.

Results and Discussion

Charge and Discharge Characteristics of $Na_{0.7}CoO_2$/Na and $Na_{0.7}CoO_2$/$Na_{15}Pb_4$ Cells

The open circuit potential of Na/P(EO)$_8$NaTf/$Na_{0.7}CoO_2$ cells is approximately 2.8 V (slightly lower when $Na_{15}Pb_4$ anodes are used). The cells were assembled in the half-discharged state, and are charged initially. Figure 1 shows a single galvanostatic charge and discharge for the cases with Na and $Na_{15}Pb_4$ anodes respectively. The extent of intercalation, x in Na_xCoO_2, was calculated based upon the amount of charge passed and corresponds to Δx =0.5 - 0.6. An assumption was made that the only process occurring during charge or discharge is electrochemical intercalation or de-intercalation. In many cases, the calculated x deviated slightly from the expected range of x = 0.3 -0.9. This was attributed to a variation of the true stoichiometry of the synthesized sodium cobalt bronze from that expected based upon the proportions of the starting materials. No attempt was made to correct for this in the voltage curves. The discharge curves appear quite similar to those obtained for P2 sodium cobalt bronze cells with liquid electrolytes at room temperature[5]; they are quite sloping and show several small steps. Plateaus are typically associated with a two phase region (i.e., a phase transition) and sloping curves with changes of composition of a single phase. However, no evidence for phase change has been found for this material over this range of intercalation; instead, the presence of steps in the voltage profiles has been attributed to ordering transitions. Although the solid polymer

electrolyte cells are operated at higher temperatures (90-100° C) than those with liquid electrolytes, the similarities in discharge characteristics strongly suggest the existence of a single phase under these conditions as well. Furthermore, previous structural studies on the sodium cobalt bronzes indicate that interchange between the P2 and other phases occurs with difficulty and only at temperatures above 700° C.

Figure 2 shows one cycle of an $Na_{15}Pb_4$/P(EO)$_8$NaTf/Na_xCoO_2 cell that was overcharged (corresponding to the removal of Na to composition $Na_{0.1}CoO_2$). The subsequent discharge showed that this process was irreversible. It was possible to cycle this cell, but the discharge capacity was decreased. In all likelihood, it is not possible to remove sodium ions in the P2 sodium cobalt bronze beyond a composition of $Na_{0.3}CoO_2$ without disrupting the structure. Therefore, in order to obtain good cycling results, some care had to be taken in choosing the upper voltage limit. (Cyclic voltammetry experiments in this laboratory show that P(EO)$_8$NaTf is stable to at least 4.2 V vs. Na[9], but lower voltage limits than this were chosen to minimize over-extraction of sodium ions from the bronze.)

Figure 3 shows discharge curves at different current densities up to 2.5 mA/cm^2 for Na/P(EO)$_8$NaTf/$Na_{0.7}CoO_2$ cells. The rate capability of this system is clearly quite high. In fact, the entire capacity of the cell can be discharged as well as charged in under an hour at 0.5 mA/cm^2, and 2.5 mA/cm^2 can be sustained for several minutes, corresponding to a 25% depth of discharge. Similar behavior is seen when sodium/lead alloy anodes are used.

Cycling Results

Cycling results show that the P2 sodium cobalt bronze is very reversible when used in sodium or sodium/lead alloy SPE cells. Figure 4 shows capacity as a function of cycle number for an example discharged and charged at 0.5 mA/cm^2 continuously two hundred times. A rapid decrease in capacity is seen initially, but then the utilization levels out at more than 60% thereafter. This capacity fading is typical of all of the cells that were cycled under these conditions. Some of the capacity decrease may be attributed to mass transfer effects; when cells were allowed to rest between cycles for several hours or discharged at lower current densities, the capacity of the subsequent cycle increased (but not to the level seen initially). Figure 5 shows the charge efficiency for the same cell, defined as the ratio of coulombs passed during charge to that passed during discharge. For most cycles this is close to one, but occasional overcharges are necessary to compensate for dendritic shorting during the charge process. (This is manifested as a voltage instability during charge.) Usually, overcharging below 4.0 V corrects the capacity loss associated with this phenomenon. However, after cycle 110 for this example, there was a dramatic decrease in capacity from which it was not possible to recover, in spite of overcharging.

Besides the obvious decrease in capacity, a change in the shape of the discharge curve as cycling progresses is evident (Figure 6). In particular, a long plateau at about 2.2-2.3 V appears as early as the 50th cycle. To test the

hypothesis that structural changes in the cathode cause this modification in the voltage profile, x-ray diffraction experiments were performed on cathodes that had been cycled to failure, and were compared to those obtained on fresh cathodes. However, no differences were seen. While x-ray diffraction may be able to detect gross structural modifications, it is not certain whether subtle changes (such as increases in the number of defect sites) would be discernible. Another possible explanation is that the sodium cobalt oxide reacts very slowly (perhaps with the polymer electrolyte), to give a product that is undetectable in the x-ray experiment, but that has some (diminished) electrochemical activity.

Inadvertent rises in temperature occurred during some experiments, causing the sodium anodes to melt (the melting point of Na is 97° C). Although this sometimes caused shorting, there seemed to be no other deleterious effects. In fact, cells that had completely shorted (voltages read 0) could often be rendered functional again simply by removing excess sodium, lowering the temperature and recharging. Complete recovery often occurred after several cycles.

Dendrite formation generally occurs less frequently in cells with sodium/lead anodes, and overcharging is not required as often as with pure sodium. Another advantage to the sodium/lead anode is its higher melting point, allowing a greater temperature range of operation. Two hundred medium to shallow depth cycles ($\Delta x = 0.1$ -0.4 in Na_xCoO_2) have been obtained for a cell with a $Na_{15}Pb_4$ anode. (Figures 7 and 8). This is the same cell that was overcharged to composition $Na_{0.1}CoO_2$ (Figure 2). The effect of various voltage limits on performance is also shown. Whereas overcharging above 4.0 V tended

to cause a decrease in capacity, cells are relatively impervious to over discharge and can withstand low voltage cutoffs.

Cells with two sodium cobalt bronze electrodes of matched capacity and a polymer electrolyte separator were also assembled and tested. Initially, the voltage is 0, but rises to 2.0 V upon charge, or drops to -2.0 V upon discharge. This corresponds to a total range of intercalation equivalent to $\Delta x = 0.6$. (Again, there was a slight deviation of stoichiometry from the range expected.) Because $Na_{0.7}CoO_2$ is approximately halfway discharged, one electrode acts as a sodium ion acceptor and the other as a sodium ion donor upon passage of current. The overall half-cell reaction for the theoretical range is shown below.

$$1) \qquad Na_{0.3}CoO_2 + 0.6\,Na^+ + 0.6\,e^- \longleftrightarrow Na_{0.9}CoO_2$$

Figure 9 shows the results of three hundred cycles at 0.5 mA/cm^2. For this example, capacity fading is clearly seen which can be attributed mainly to processes occurring in the sodium cobalt bronze electrode, in the polymer electrolyte and/or in the interfaces of the cathode with the polymer electrolyte and current collectors, rather than at the sodium/PEO interface. The effect may be due to mass transfer phenomena, chemical or structural changes in the sodium cobalt bronze or modifications in the structure of the composite positive electrode. AC impedance studies[10] on cycled intercalation electrodes show an increase in resistance that has been attributed to disconnection processes rather than structural changes in the electroactive material. The volume expansion and contraction associated with the insertion and de-insertion of ions may cause exfoliation and

cracking of the electroactive particles and concomitant disruption of the paths for electronic and/or ionic conductivity in the composite electrode. Not only does the isolation of the electroactive particles lead to lowered capacity and increased resistance, but loss of interfacial contact may also result.

While dendritic shorting certainly may cause premature failure, the sodium electrode or sodium/PEO interface does not seem to be a major cause of capacity fading. (Further evidence for this is presented in the next section). While more study is needed to determine how much each of the factors discussed above contributes to cycle life, it should be possible to improve performance simply based upon the information already obtained. Changes in the composition of the electrolyte may improve conductivity or minimize reaction with the sodium cobalt bronze. Modifications in the fabrication of the composite electrodes (varying the amount or type of electronically conducting additive, loading levels, etc.) or in the way the cell is assembled may dramatically improve cyclability particularly if disconnection or loss of interfacial contact is occurring.

Four Probe DC Experiments

To determine how the various components in the $Na/P(EO)_8NaTf/Na_xCoO_2$ system contribute to performance, cells with two sodium foil reference electrodes were constructed and tested. These were referred to the sodium anode. A polymer electrolyte layer separates each electrode for a total of three in the cell. A simple arithmetic procedure then allows calculation of the overpotentials for each component (i.e., the cathode, the polymer electrolyte, and the Na/PEO interface) during galvanostatic charge and discharge or pulsing[8].

Because it is performed *in situ,* this experiment can provide a great deal of information about processes occurring during conditions of actual cell use.

Sequential bipolar square-wave current pulses were applied to the four probe cell and the response of the overall cell potential and the reference electrodes were recorded. This allows determination of the contribution of the various components to the resistance of the cell with a minimum of disturbance to the system. The pulse time was chosen to minimize complications due to mass transport and double layer charging. Subtraction of the response of reference 1 (the electrode closest to the negative) from that of reference 2 gives the resistance due to the polymer electrolyte (ohmic response). The reference 1 response less the ohmic response gives the resistance due to Na and the Na/PEO interface, and the overall cell overpotential less the response of reference 2 and the ohmic response gives the resistance due to the cathode. Results of this experiment performed after the second cell discharge are shown in Figure 10. By far the major contributor to overall cell resistance under these conditions is the cathode (52.5 Ω), as might be expected. The polymer electrolyte (2.0 Ω) and the sodium and sodium/PEO interface (4.2 Ω) make only minor contributions to cell resistance.

The four-probe method can also be applied to cells undergoing galvanostatic charge or discharge. The end of discharge or charge is marked by a dramatic increase in the cell overpotential, dominated strongly by the cathode polarization. The sodium/PEO interface resistance is so low as to be nearly undetectable throughout the course of the experiment. There is, however, an initial increase in the resistance of the PEO electrolyte as charging or discharging progresses (Figure 11), which then levels to a constant value. This was seen for all of the four probe discharge and charges over several cycles, and marks the transition to single ion conduction. In this regard, it is equivalent to experiments in which a cell is potentiostatically polarized, and the resultant decay in current measured in order to calculate transference numbers. These results give a value of about $t_+ = 0.13$ for sodium ions in $P(EO)_8NaTf$ under these conditions. Accurate measurement and interpretation of transference numbers in PEO complexes is a complicated issue[11], but growing evidence shows that anions tend to be more mobile than cations in PEO[12].

Figure 12 shows the change in resistance of the various cell components as a function of the cycle number, determined by pulsing after charge or discharge. It is clear that the electrolyte and sodium/PEO interface contribute only slightly, if at all, to the overall resistance increase seen in the cell in the first few cycles. Clearly, this process is dominated by the cathode resistance. Previous AC impedance results on $Na/P(EO)_8NaClO_4$ systems[13], in contrast, suggest that corrosion at the sodium/electrolyte interface is the major factor contributing to increasing cell resistance upon cycling. Corrosion processes, however, are expected to be highly dependent upon the purity of the sodium and dryness of

components. Results of AC experiments can also be quite different from those obtained during DC polarization of cells. Indeed, the high interfacial impedances that were seen in the study by West et al.[13] always decreased upon passage of a DC current, suggesting that the corrosion layer breaks down upon cell polarization. The four probe experiments, the cycling results on Na and $Na_{15}Pb_4$/P(EO)$_8$NaTf/Na_xCoO_2 cells, and the cycling results on positive/positive cells all indicate that the sodium/PEO interface is stable in these cells and that the cycle life is primarily determined by the cathode.

Figure 12 also shows that the cathode resistance is consistently higher after discharge than after charge. This suggests that the conductivity of Na_xCoO_2 increases with decreasing x, or that there is a consistent change in the particle connectivity due to the volume changes occurring during the intercalation and de-intercalation processes.

Power and Energy Density Calculations

High theoretical volumetric energy densities of 1600 and 1470 Wh/L are calculated for the P2 sodium cobalt bronze with sodium and sodium/lead alloy anodes respectively, based upon the discharge characteristics and measured density of 4.81 g/cc. The theoretical gravimetric energy densities of 440 Wh/kg for Na and 350 Wh/kg for $Na_{15}Pb_4$ also could meet the requirements of electric vehicle batteries. In cells with liquid electrolytes, it is usually possible to attain practical energies of about one-fourth that of the theoretical. One advantage to using solid state components, however, is that light weight ultra thin current collectors may be used to maximize practical energy densities, because there is no

danger of electrolyte leakage[14]. To illustrate this, practical energy densities were estimated, assuming 5 μm metallized plastic current collectors with sodium cobalt bronze electrodes, 10 μm thick polymer electrolyte separators and a two-fold excess of sodium are used, and are given in Figure 13. These calculations show that up to 150 Wh/kg for this configuration is attainable, depending upon the loading level and capacity of the positive electrode. It may be possible to increase this further, by increasing the loading level in the cathode to 60%, but this has not yet been tested for the sodium cobalt bronze.

Practical power densities based upon the configuration described above and the data shown in Figure 3 are presented in Figure 14. At 0.5 mA/cm^2, the entire capacity of the positive electrode can be discharged in less than an hour (varying somewhat depending upon the cell capacity). This corresponds to a practical power density of 335 W/L for continuous operation. Up to 2.7 kW/L is attainable for short periods of time (several minutes) for a depth of discharge of 25% of the available capacity in the positive.

Because less capacity can be discharged at higher current levels, cells designed for high rate and thus high power density applications should use thinner electrodes (i.e., fewer coulombs per unit area in the cathode). If energy density is the primary consideration, cells with larger capacities should be built. The Ragone plot presented in Figure 15 indicates the relationship between energy and power densities. For electric vehicle applications, both high energy densities and high power densities for at least short periods of time are important attributes. It appears that the Na_xCoO_2/$P(EO)_8$NaTf/Na system has the potential for fulfilling these requirements.

Conclusions

Na_xCoO_2/P(EO)$_8$NaTf/Na and $Na_{15}Pb_4$ cells have been evaluated in terms of discharge characteristics, rate capability, cyclability and power and energy densities. One hundred cycles to 60% depth of discharge or betterat 0.5 mA/cm^2 and two hundred shallower cycles at the same rate have been obtained . Experiments in which positive/positive cells were cycled suggest that the limits to cyclability lie with the cathode and not with the Na/PEO interface, but x-ray diffraction experiments failed to reveal any structural changes in the sodium cobalt bronze itself. Four probe DC experiments also show that the major contribution to overall cell resistance is in the cathode, and that there is little or no change of the Na/PEO interfacial characteristics with cycling. Loss of interfacial contact, disconnection in the cathode, chemical or structural changes in the sodium cobalt bronze and mass transfer effects are suggested as factors contributing to eventual cell failure, but more exploration is needed. In terms of cyclability, theoretical energy density and rate capability, these are the best results obtained on a sodium/polymer electrolyte system to date. Furthermore, energy and power density projections show that Na_xCoO_2/PEO/Na batteries may meet the requirements for electric vehicle use. The low cost of sodium relative to lithium makes sodium polymer batteries an attractive alternative for these and other applications.

Acknowledgment

This work was supported by the Assistant Secretary for Conservation and Renewable Energy, Office of Transportation Technologies, Electric & Hybrid Propulsion Division of the U.S. Department of Energy under Contract No. DE-AC03-76SF00098.

References

[1] K. West, B. Zachau-Christiansen, T. Jacobsen and S. Atlung, *J. Electrochem. Soc.*, **132**, 3061 (1985).

[2] R. Koksbang, S. Yde-Andersen, K. West, B. Zachau-Christiansen and S. Skaarup, *Solid State Ionics*, **28-30**, 868 (1988).

[3] a) K. West, B. Zachau-Christiansen, T. Jacobsen and S. Skaarup, *Solid State Ionics*, **28-30**, 1128 (1988).

b) J. Y. Cherng, M. Z. A. Munshi, B.B. Owens and W. H. Smyrl, *Solid State Ionics*, **28-30**, 857 (1988).

c) M. Z. A. Munshi, A. Gilmour, W. H. Smyrl, and B. B. Owens, *J.Electrochem. Soc.*, **136**, 1847 (1989).

d) M. Z. A. Munshi and W. H. Smyrl, *Solid State Ionics.*, **45**, 183 (1991).

e) G. Wang and G. Pistoia, *J. Electroanal. Chem.*, **302**, 275 (1991).

[4] *Handbook of Chemistry and Physics, 71st edition*, R.C. Weast, M. J. Astle and W. H. Beyer eds. CRC press, Inc. Boca Raton, Florida 1992.

[5] L. W. Shacklette, T.R. Jow and L. Townsend, *J. Electrochem. Soc.*, **135**, 2669 (1988).

[6] C. Delmas, J-J. Braconnier, C. Fouassier, and P. Hagenmuller, *Solid State Ionics*, **3/4**, 165 (1981).

[7] S. Miyazaki, S. Kikkawa, and M. Koizumi, *Synthetic Metals*, **6**, 211 (1983).

[8] M. Liu, S. J. Visco and L. C. De Jonghe, *Electrochimica Acta-Special Issue on Lithium Batteries* accepted for publication.

[9] unpublished results.

[10] R. Koksbang, I. I. Olsen, P. E. Tonder, N. Knudsen and D. Fauteux, *J. Applied Electrochemistry*, **21**, 301 (1991).

[11] a) P. G. Bruce and C. A. Vincent, *Solid State Ionics*, **40/41**, 607 (1990).

b) J. Evans, C. A. Vincent and P. G. Bruce, *Polymer*, **28**, 2324 (1987).

c) G. G. Cameron, J. L. Harvie and M. D. Ingram, *Solid State Ionics*, **34**, 65 (1989).

d) A. Bouridah, F. Dalard, D. Deroo and M. B. Armand, *Solid State Ionics*, **18&19**, 287 (1986).

e) A. Bouridah, F. Dalard, D. Deroo and M. B. Armand, *J. Applied Electrochem.*, **17**, 625 (1987).

[12] a) M. Armand, *Solid State Ionics*, **8&10**, 745 (1983).

b) *Electroresponsive Molecular and Polymeric Systems*, Vol. 1, T. A. Skotheim, Editor, Chap. 2, Marcel Dekker, Inc., New York (1988).

c) P. Ferloni, G. Chiodelli, A. Magistris, and M. Sanlesi, *Solid State Ionics*, **18&19**, 265 (1986).

d) M. M. Doeff, M. M. Lerner, S. J. Visco, and L. C. De Jonghe, *J. Electrochem. Soc.*, **139**, 2077 (1992).

[13] K. West, B. Zachau-Christiansen, T. Jacobsen, E. Hiort-Lorenzen and S. Skaarup, *Brit. Polymer Journal*, **20**, 243 (1988).

[14] a) M. Z. A. Munshi and B. B. Owens, *Solid State Ionics*, **38**, 87 (1990).

b) M. Z. A. Munshi and B. B. Owens, *ibid.*, **38**, 95 (1990).

c) M. M. Doeff, S. J. Visco, and L. C. De Jonghe, *J. Electrochem. Soc.*, **139** 1808 (1992).

Table 1. Characteristics of Anode Materials for Polymer Batteries

Characteristic	Na	Li
Cost/equiv. (dollars) for Bulk Metal	0.01	0.54
Capacity Density (Ah/g)	1.16	3.86
V vs. S.H.E	-2.7	-3.0
Ionic radius (Å)	0.98	0.68

Figure Captions

Figure 1. Cell potentials vs. x in Na_xCoO_2 in a) a cell with a sodium anode at 90° C and b) a cell with an $Na_{15}Pb_4$ anode at 100° C. The current density was 0.5 mA/cm^2 for both charge and discharge. Voltage was plotted as a function of x in Na_xCoO_2 based upon the amount of charge passed.

Figure 2. Overcharge of an $Na_{15}Pb_4/P(EO)_8NaTf/Na_xCoO_2$ cell (cutoff potential 4.0 V). The subsequent discharge showed reduced capacity. The charge current density was 0.1 mA/cm^2 and the discharge current density was 0.2 mA/cm^2.

Figure 3. Discharge curves at various current densities up to 2.5 mA/cm^2 for $Na/P(EO)_8NaTf/Na_{0.7}CoO_2$ cells at 90° C.

Figure 4. Capacity as a function of cycle number for a $Na/P(EO)_8NaTf/Na_xCoO_2$ cell. The current density was 0.5 mA/cm^2 for both charge and discharge, and the temperature was 90° C.

Figure 5. Charge efficiency for the cell in Figure 4, defined as the ratio of coulombs passed during charge to that passed during discharge.

Figure 6. Discharge curves as a function of cycle number for the $Na/P(EO)_8NaTf/Na_xCoO_2$ cell from Figures 4 and 5.

Figure 7. Capacity as a function of cycle number for an $Na_{15}Pb_4/P(EO)_8NaTf/Na_xCoO_2$ cell. Various discharge and charge rates were used for the first ten cycles (these are not shown), and the cell was overcharged during the second cycle, leading to reduced capacity. A discharge and charge current density of 0.5 mA/cm^2 was used for the subsequent cycles, except as noted. The effect of various voltage limits is also shown..

Figure 8. Charge efficiency for the cell in Figure 7 defined as the ratio of coulombs passed during charge to that passed during discharge.

Figure 9. Capacity as a function of cycle number for an $Na_{0.7}CoO_2/P(EO)_8NaTf/Na_{0.7}CoO_2$ cell at 90° C. The current density was 0.5 mA/cm^2 for both charge and discharge.

Figure 10. Overpotentials of cell components and interfaces upon the application of sequential bipolar square wave pulses to a four probe cell after the second cycle at 90° C. The time for each pulse was 50 ms. Only the discharge response is shown for clarity.

Figure 11. The change in resistance of the polymer electrolyte and at the sodium electrode in a four probe cell undergoing galvanostatic discharge at 0.33 mA/cm^2. The cathode resistance as a function of time is not shown, but exactly follows that of the cell as a whole.

Figure 12. Change in resistance of components in a four probe cell as a function of cycle number, obtained from sequential square wave pulse data similar to that shown in Figure 10. The values obtained after discharge are plotted on the positive axis, and those obtained after charge are plotted on the negative axis for clarity.

Figure 13. Practical energy density as a function of loading level and capacity in the sodium cobalt bronze electrode. These calculations assume a cell being discharged at 0.5 mA/cm^2, metallized plastic current collectors 5 μm thick, PEO separators 10 μm thick, and a twofold excess of sodium in the anode.

Figure 14. Gravimetric (lower line) and volumetric (upper line) practical power densities for Na_xCoO_2/$P(EO)_8$NaTf/Na cells with 5 μm thick metallized plastic current collectors, 10 μm thick polymer electrolyte separators and a twofold excess of sodium in the anodes. The loading level in the cathode is assumed to be 45 wt. % electroactive material. The graph shows the amount of time that the corresponding currents can be sustained as well as the depths of discharge based on the data shown in Figure 3.

Figure 15. Ragone plot for Na_xCoO_2/P(EO)$_8$NaTf/Na cells, using the calculations shown in Figure 14. The cell dimensions are the same as in Figure 13, and the loading level in the cathode is assumed to be 45 wt. %. The zero power density point corresponds to the energy density of a cell with a capacity of 3 C/cm^2 in the cathode.

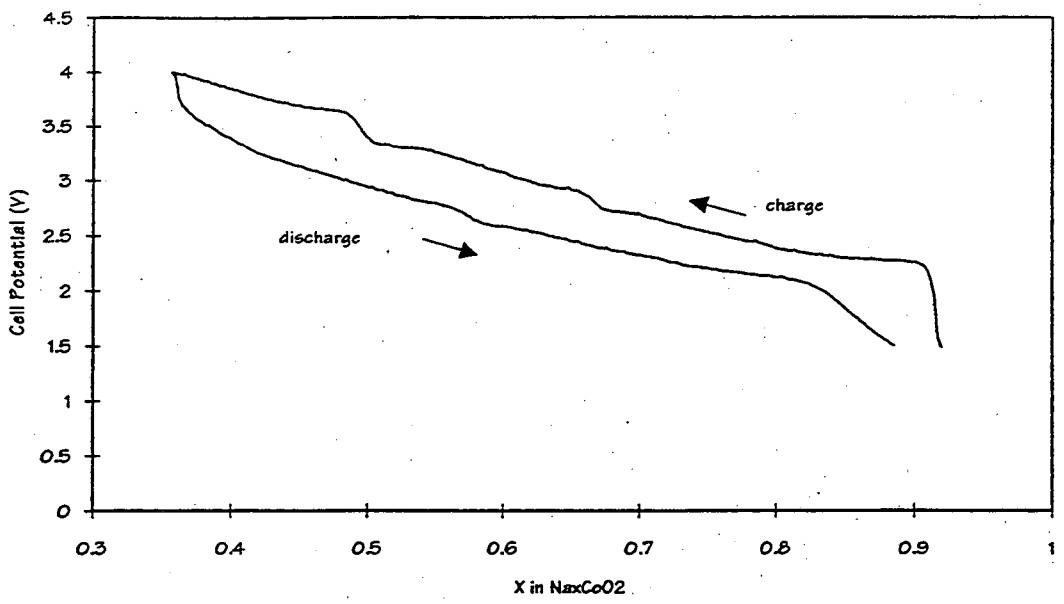
4.5
4
3.5
3
2.5
2
1.5
1
0.5
0
Cell Potential (V)
charge
discharge
0.3
0.4
0.5
0.6
0.7
0.8
0.9
1
X in NaxCo02

(a)

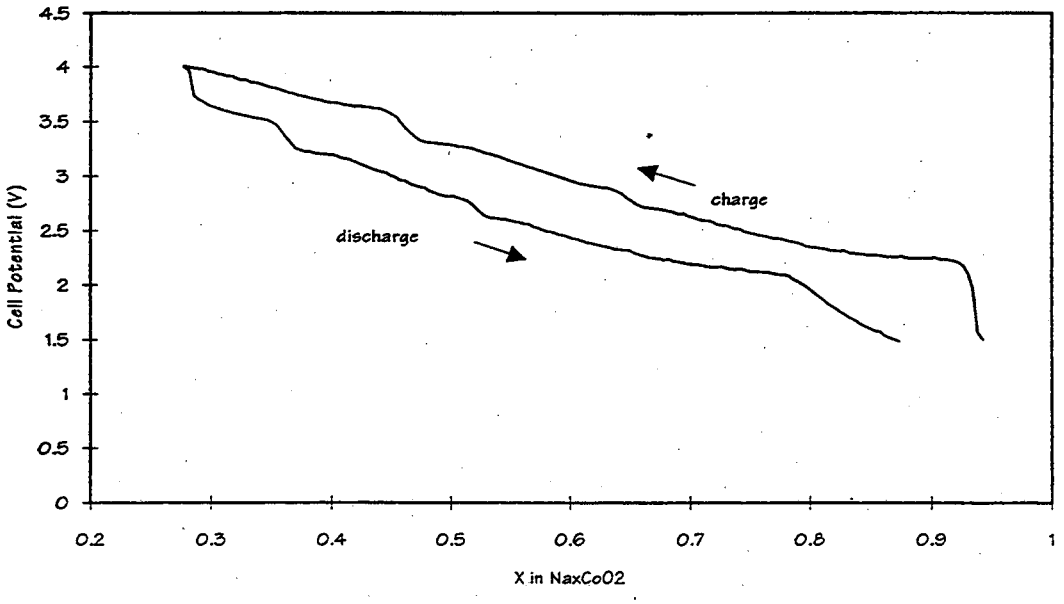
4.5
4
3.5
3
2.5
2
1.5
1
0.5
0
Cell Potential (V)
charge
discharge
0.2
0.3
0.4
0.5
0.6
0.7
0.8
0.9
1
X in NaxCo02

(b)

Figure 1

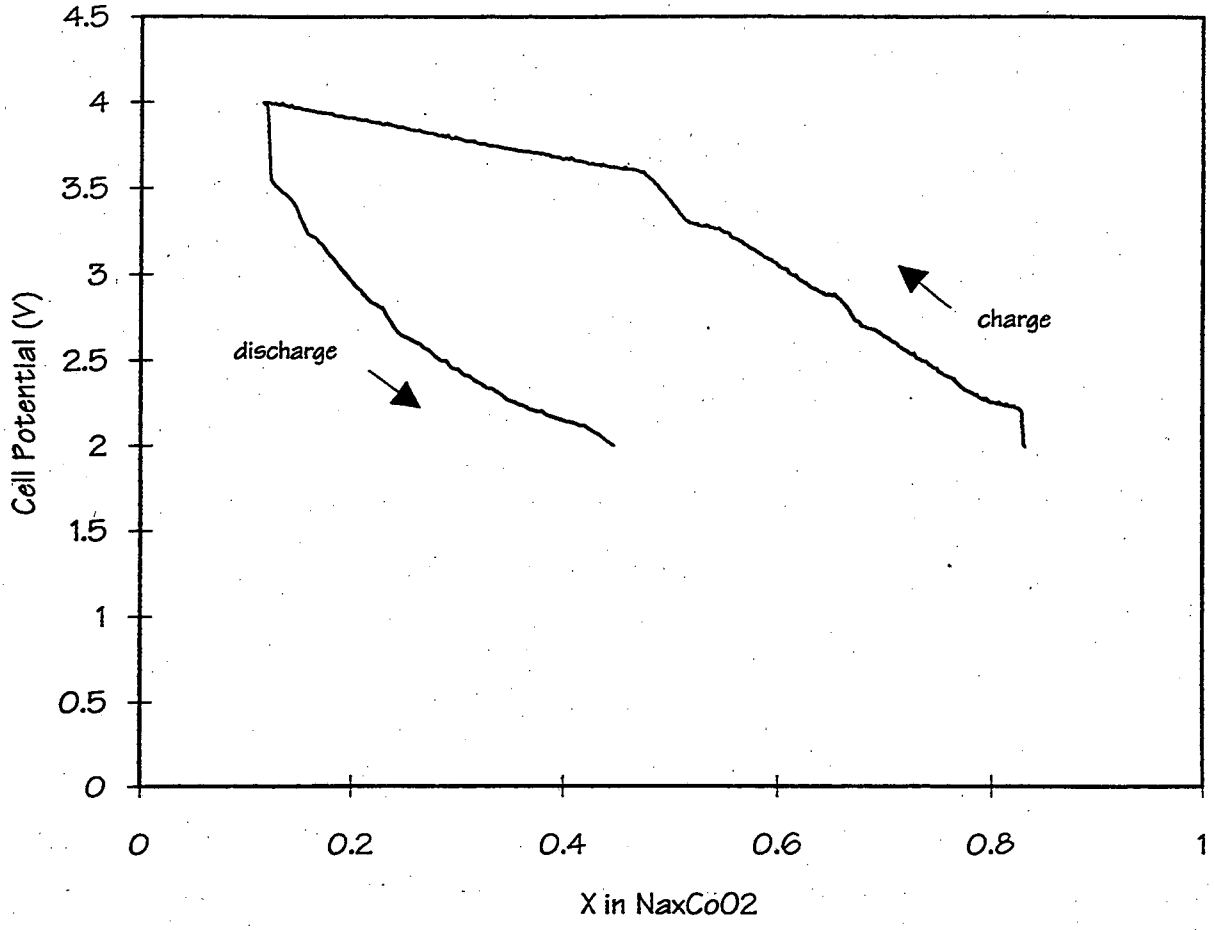
4.5
4
3.5
3
2.5
2
1.5
1
0.5
0
Cell Potential (V)
discharge
charge
0
0.2
0.4
0.6
0.8
1
X in NaxCoO2

Figure 2.

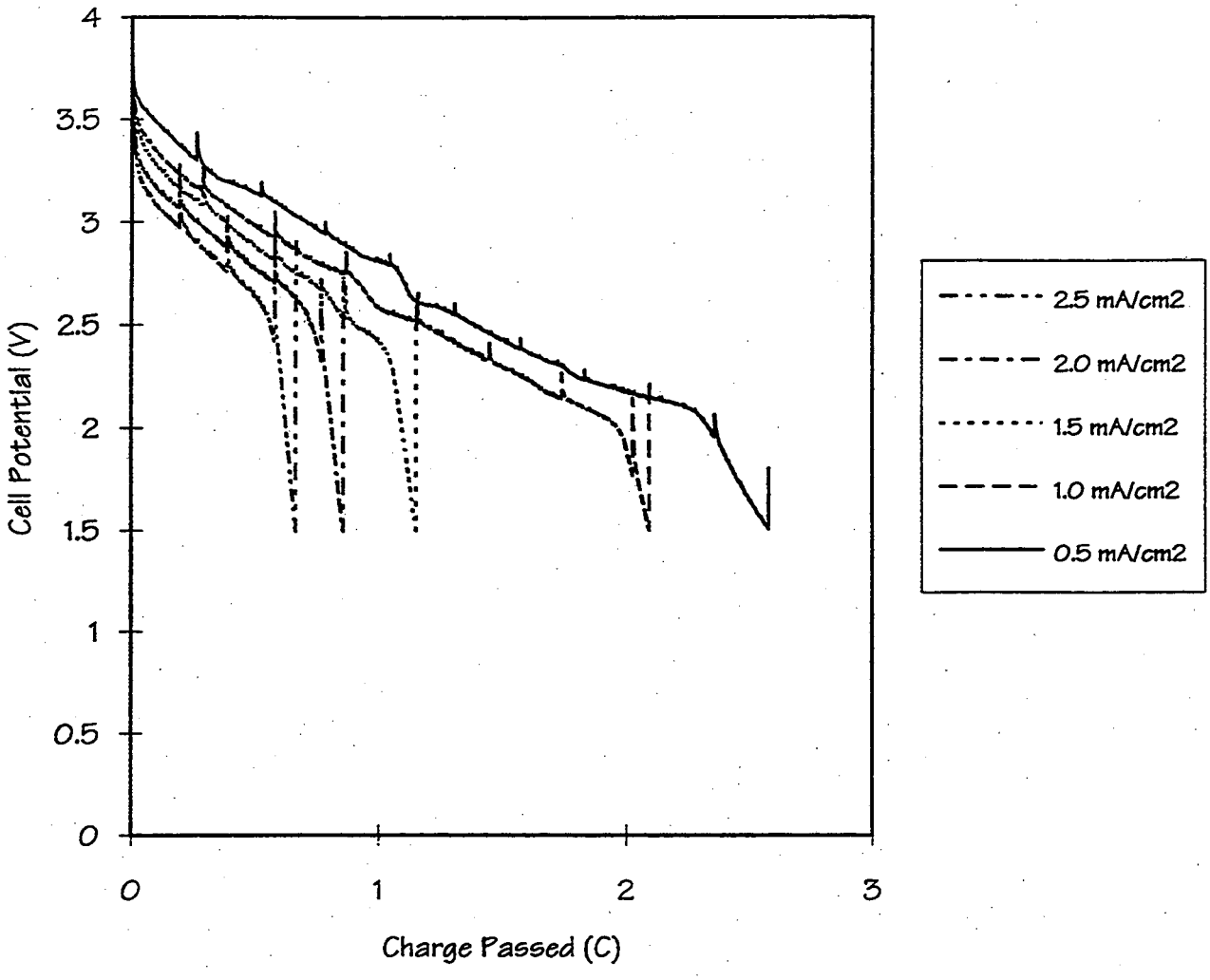
4
3.5
3
2.5
2
1.5
1
0.5
0
Cell Potential (V)
0
1
2
3
Charge Passed (C)
2.5 mA/cm2
2.0 mA/cm2
1.5 mA/cm2
1.0 mA/cm2
0.5 mA/cm2

Figure 3

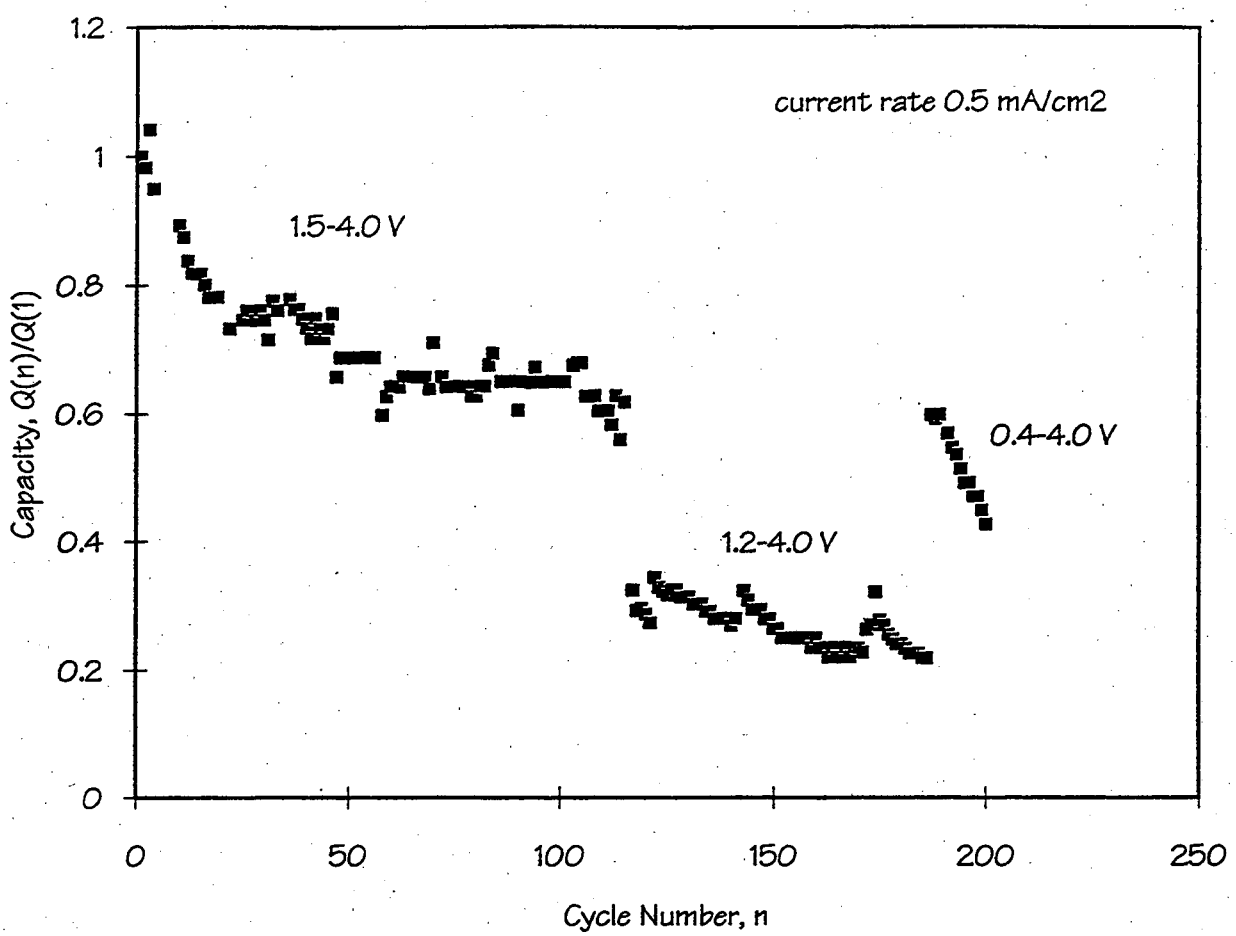
current rate 0.5 mA/cm2
1.5-4.0 V
1.2-4.0 V
0.4-4.0 V
Capacity, Q(n)/Q(1)
Cycle Number, n
1.2
1
0.8
0.6
0.4
0.2
0
0
50
100
150
200
250

Figure 4.

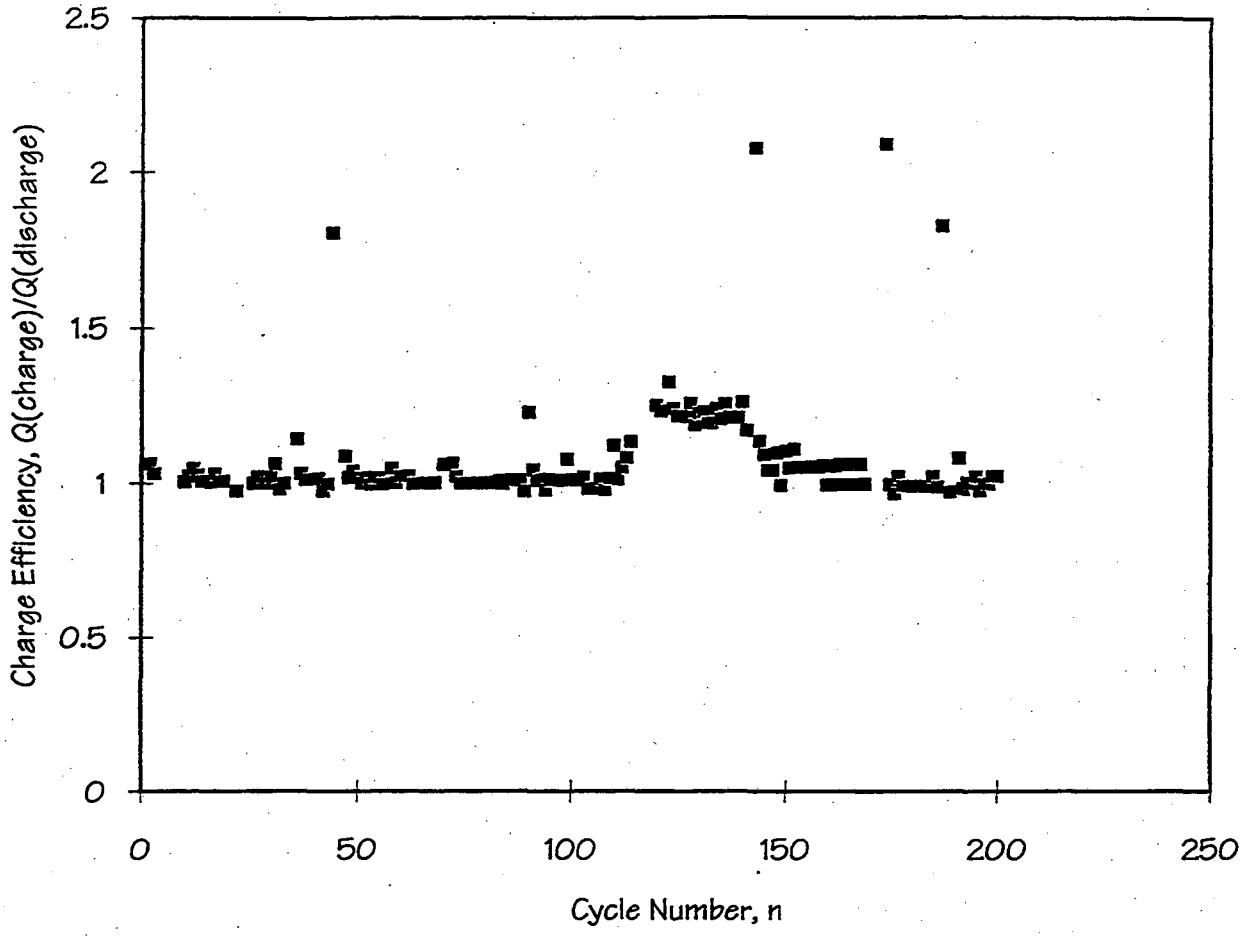
Charge Efficiency, Q(charge)/Q(discharge)
2.5
2
1.5
1
0.5
0
0
50
100
150
200
250
Cycle Number, n

Figure 5.

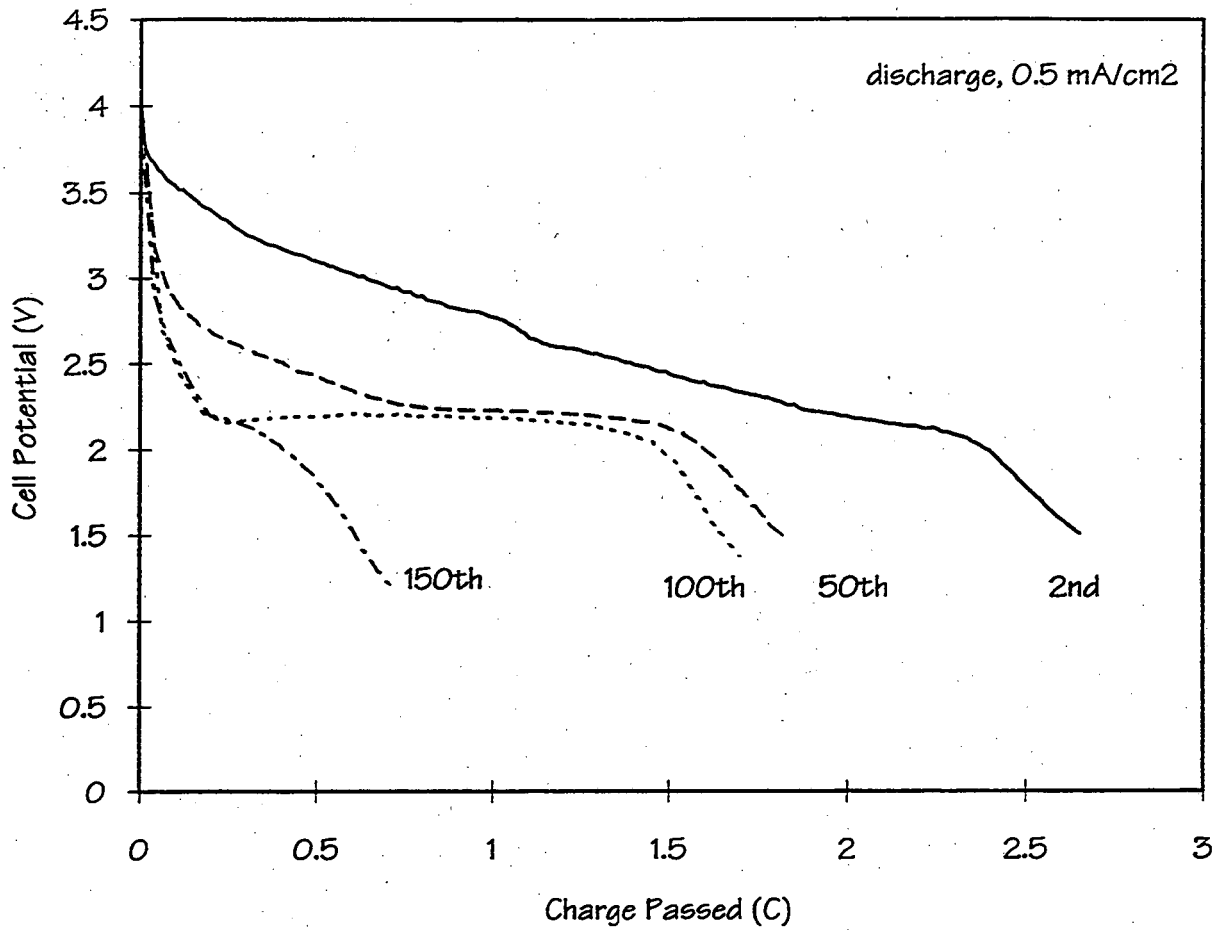
discharge, 0.5 mA/cm2
Cell Potential (V)
Charge Passed (C)
4.5
4
3.5
3
2.5
2
1.5
1
0.5
0
0
0.5
1
1.5
2
2.5
3
150th
100th
50th
2nd

Figure 6

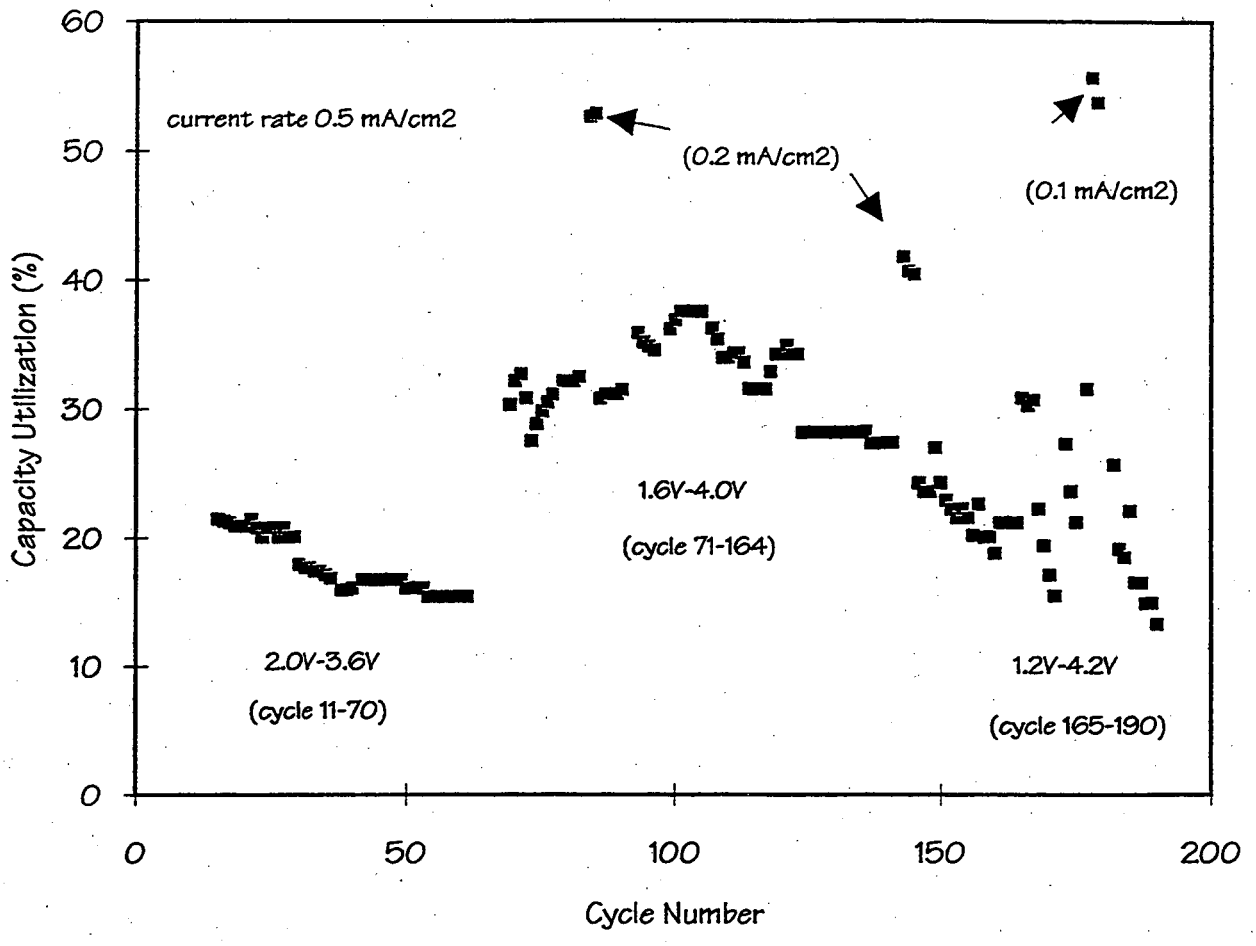
60
50
40
30
20
10
0
Capacity Utilization (%)
current rate 0.5 mA/cm2
(0.2 mA/cm2)
(0.1 mA/cm2)
1.6V-4.0V
(cycle 71-164)
2.0V-3.6V
(cycle 11-70)
1.2V-4.2V
(cycle 165-190)
0
50
100
150
200
Cycle Number

Figure 7

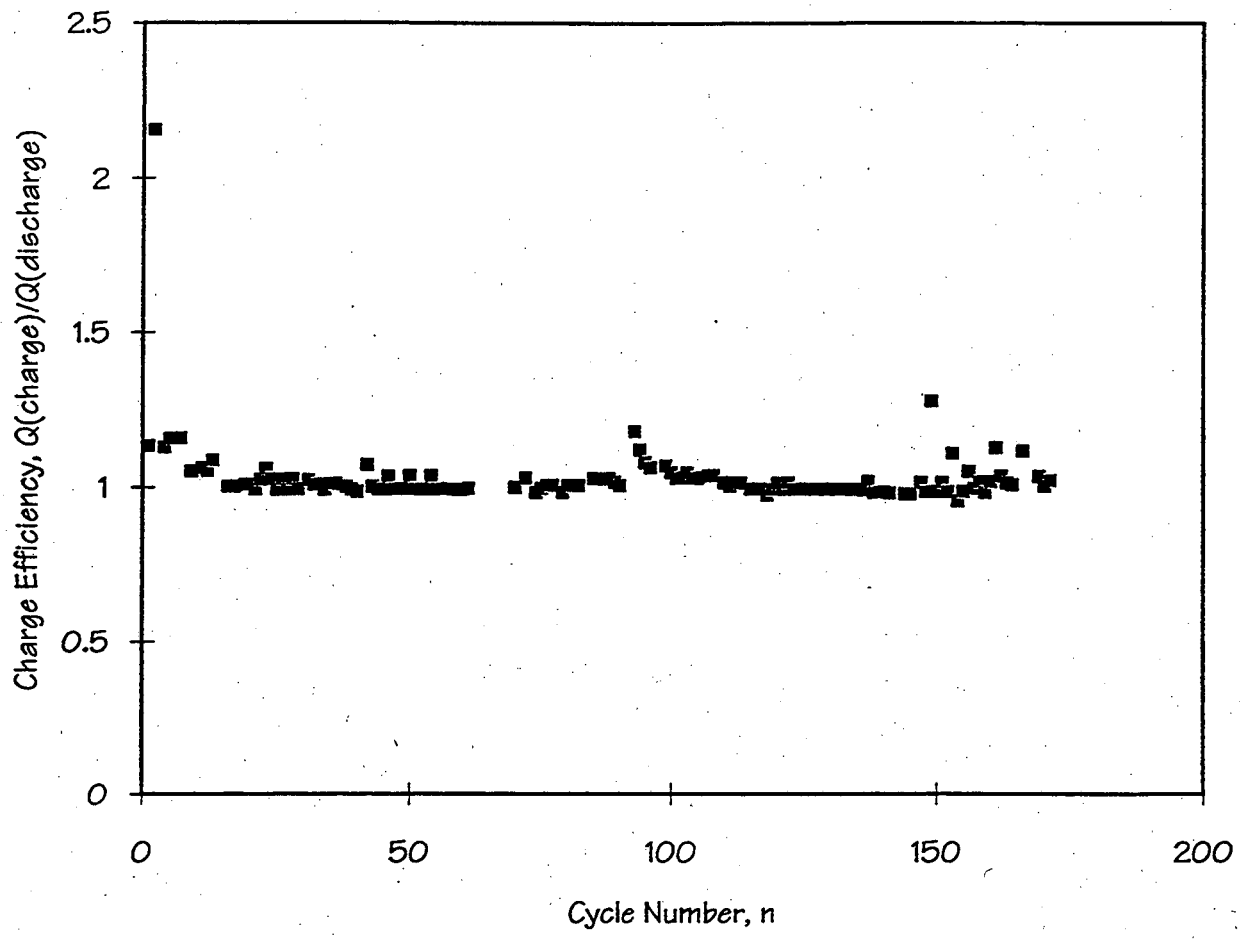
Charge Efficiency, Q(charge)/Q(discharge)
2.5
2
1.5
1
0.5
0
0
50
100
150
200
Cycle Number, n

Figure 8.

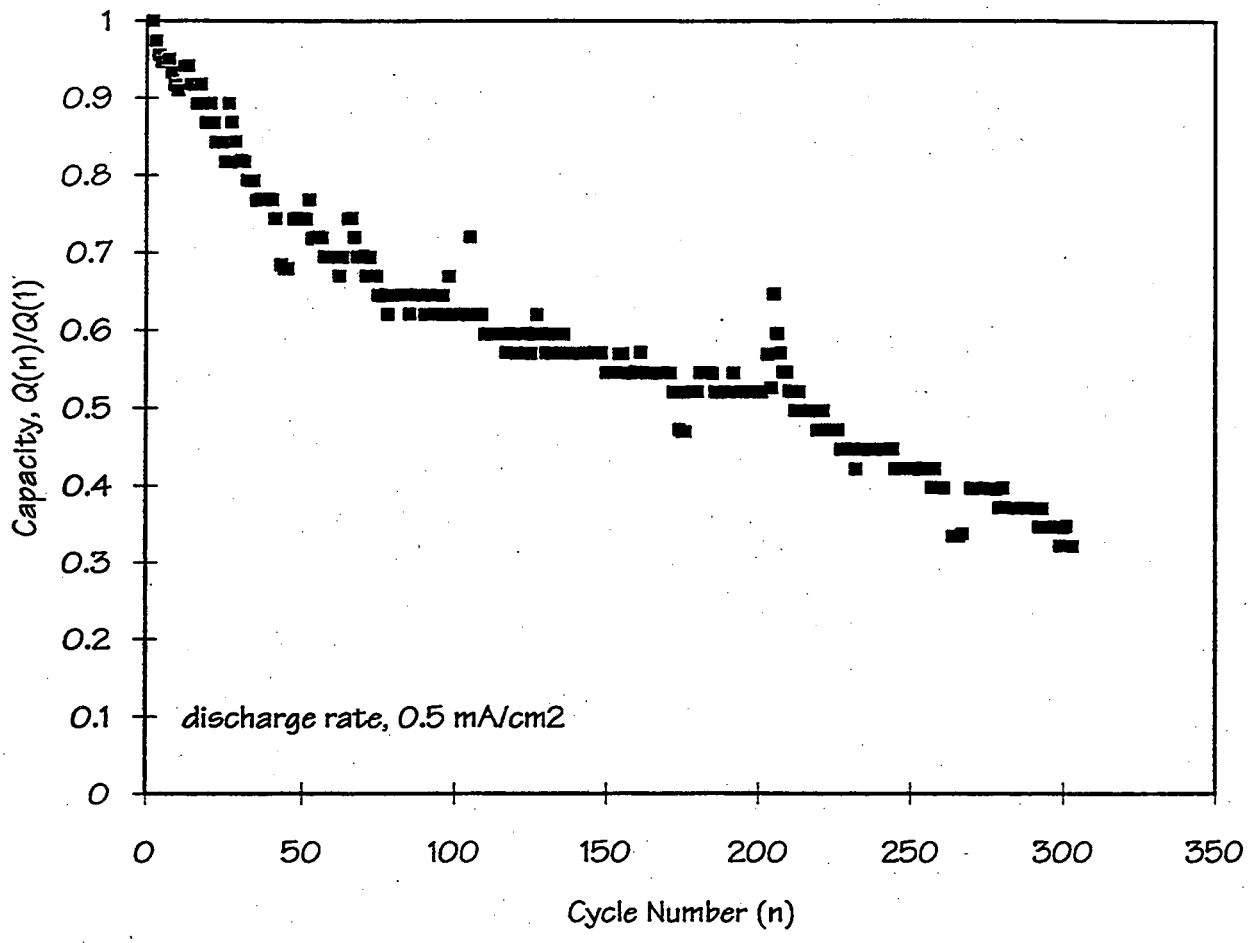
Capacity, Q(n)/Q(1)
1
0.9
0.8
0.7
0.6
0.5
0.4
0.3
0.2
0.1
0
discharge rate, 0.5 mA/cm2
0
50
100
150
200
250
300
350
Cycle Number (n)

Figure 9.

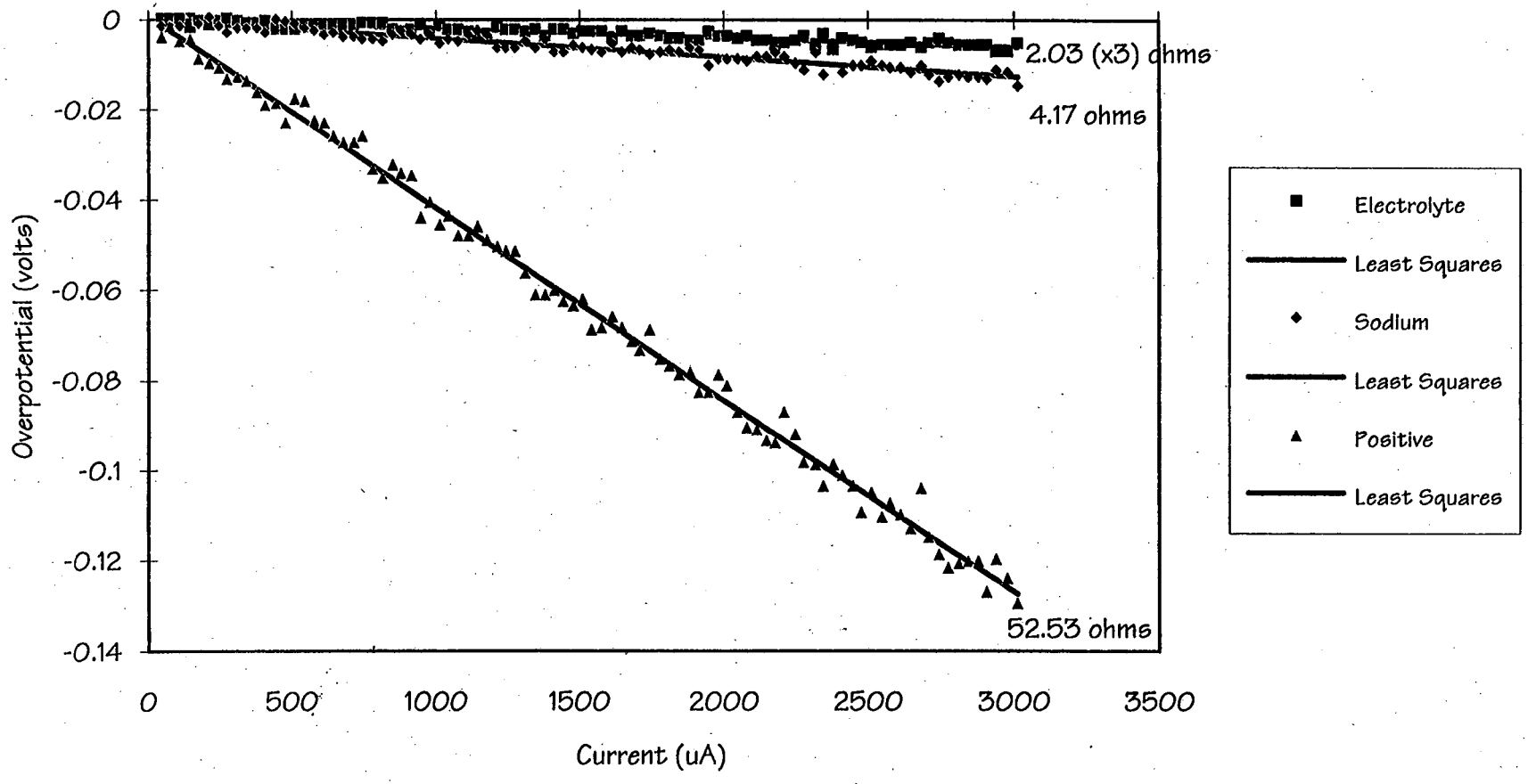
0
-0.02
-0.04
-0.06
-0.08
-0.1
-0.12
-0.14
Overpotential (volts)
0
500
1000
1500
2000
2500
3000
3500
Current (uA)
2.03 (x3) ohms
4.17 ohms
52.53 ohms
Electrolyte
Least Squares
Sodium
Least Squares
Positive
Least Squares

Figure 10

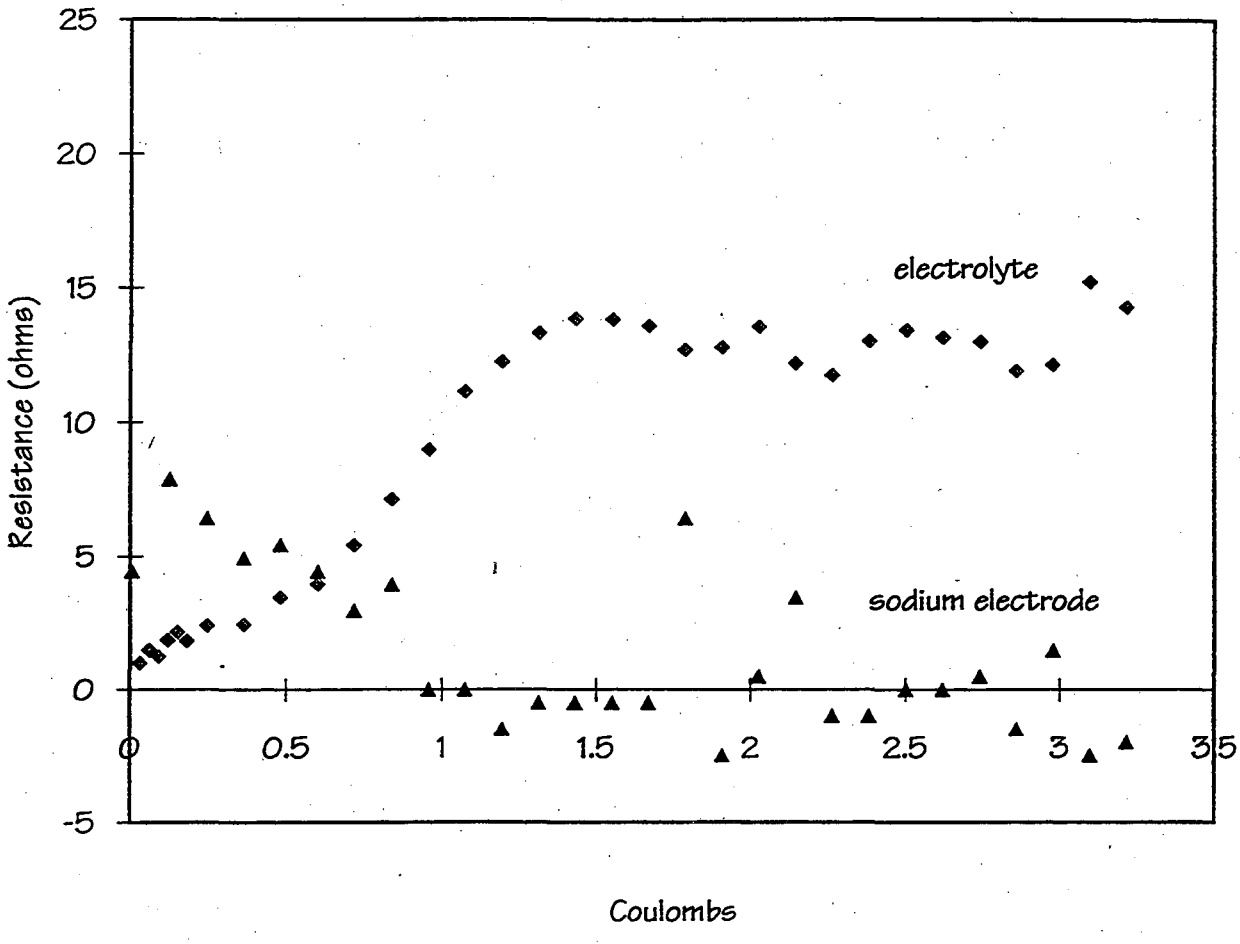
25
20
15
10
5
0
-5
Resistance (ohms)
electrolyte
sodium electrode
0
0.5
1
1.5
2
2.5
3
3.5
Coulombs

Figure 11

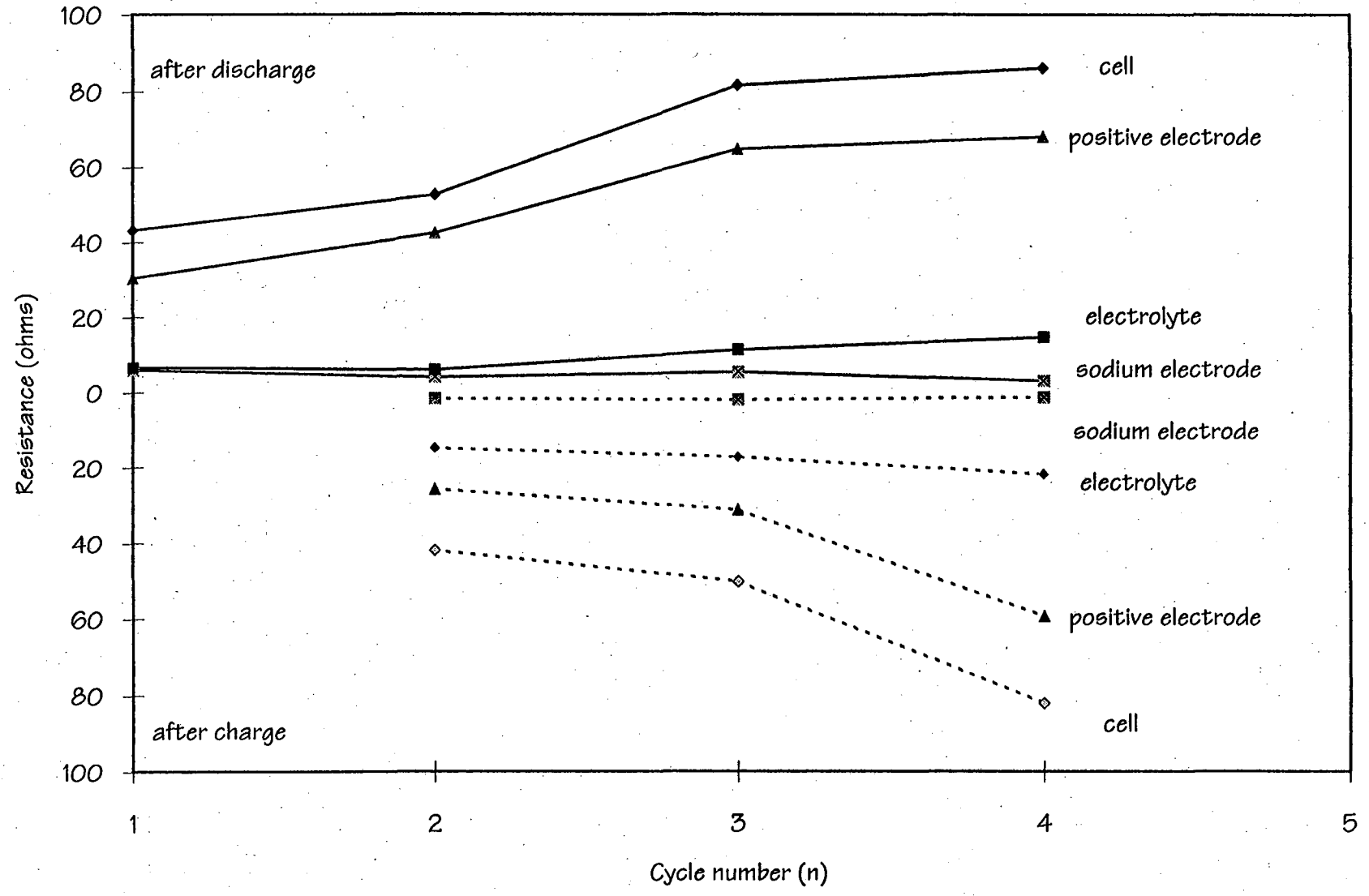
100
80
60
40
20
0
20
40
60
80
100
after discharge
after charge
Resistance (ohms)
1
2
3
4
5
Cycle number (n)
cell
positive electrode
electrolyte
sodium electrode
sodium electrode
electrolyte
positive electrode
cell

Figure 12

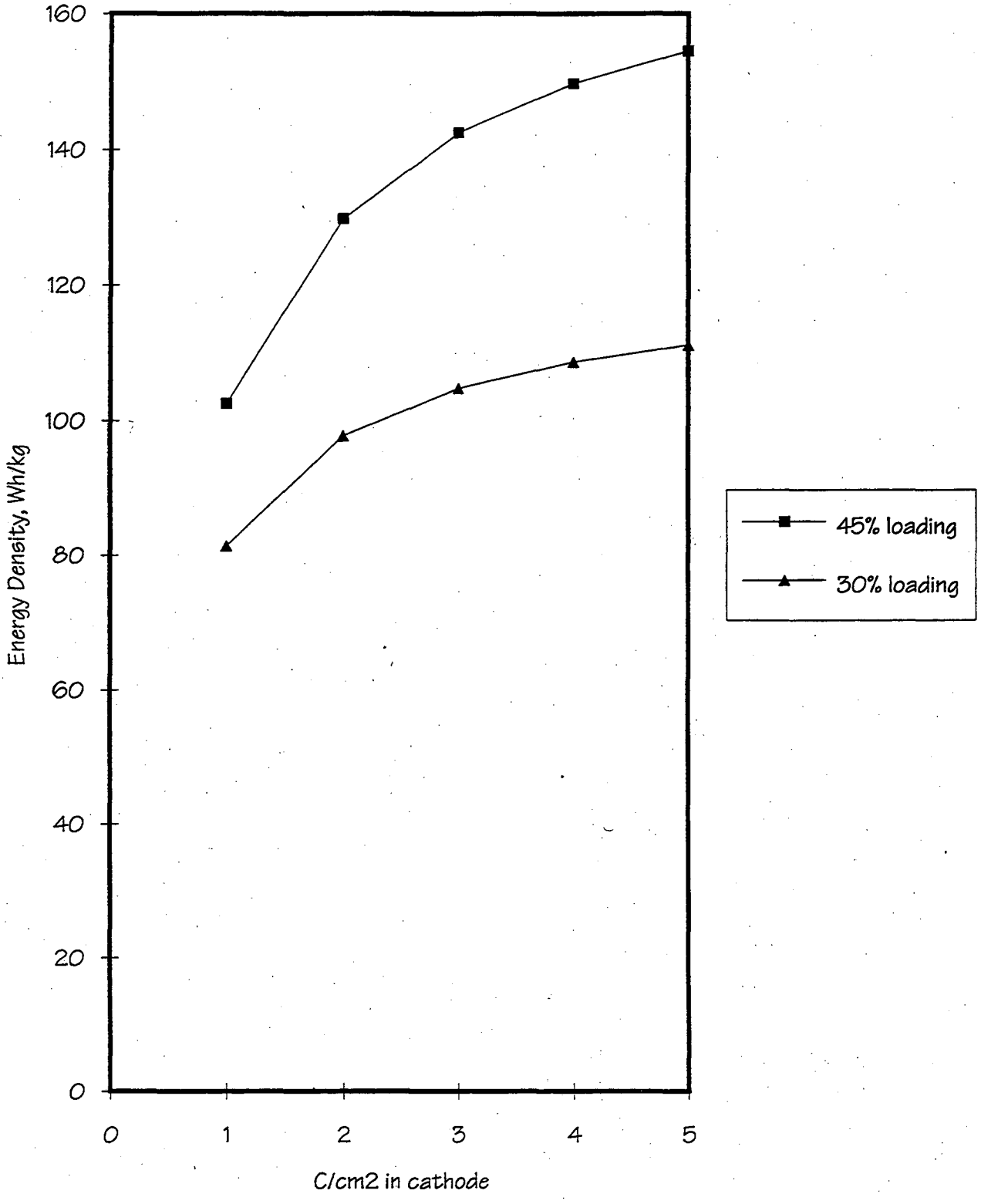
160
140
120
100
80
60
40
20
0
Energy Density, Wh/kg
0
1
2
3
4
5
C/cm2 in cathode
45% loading
30% loading

Figure 13

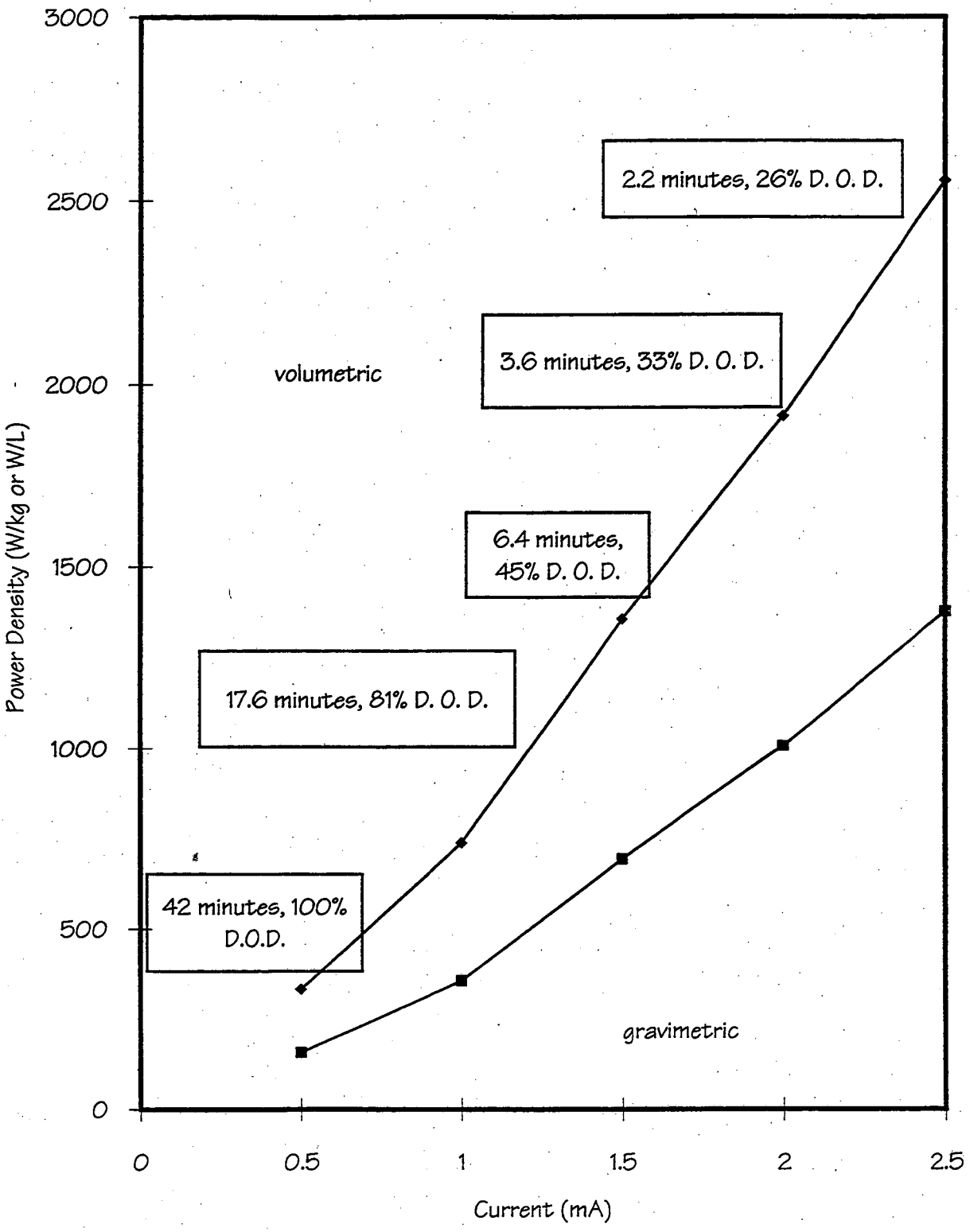
3000
2500
2000
1500
1000
500
0
Power Density (W/kg or W/L)
2.2 minutes, 26% D. O. D.
3.6 minutes, 33% D. O. D.
6.4 minutes, 45% D. O. D.
17.6 minutes, 81% D. O. D.
42 minutes, 100% D.O.D.
volumetric
gravimetric
0
0.5
1
1.5
2
2.5
Current (mA)

Figure 14

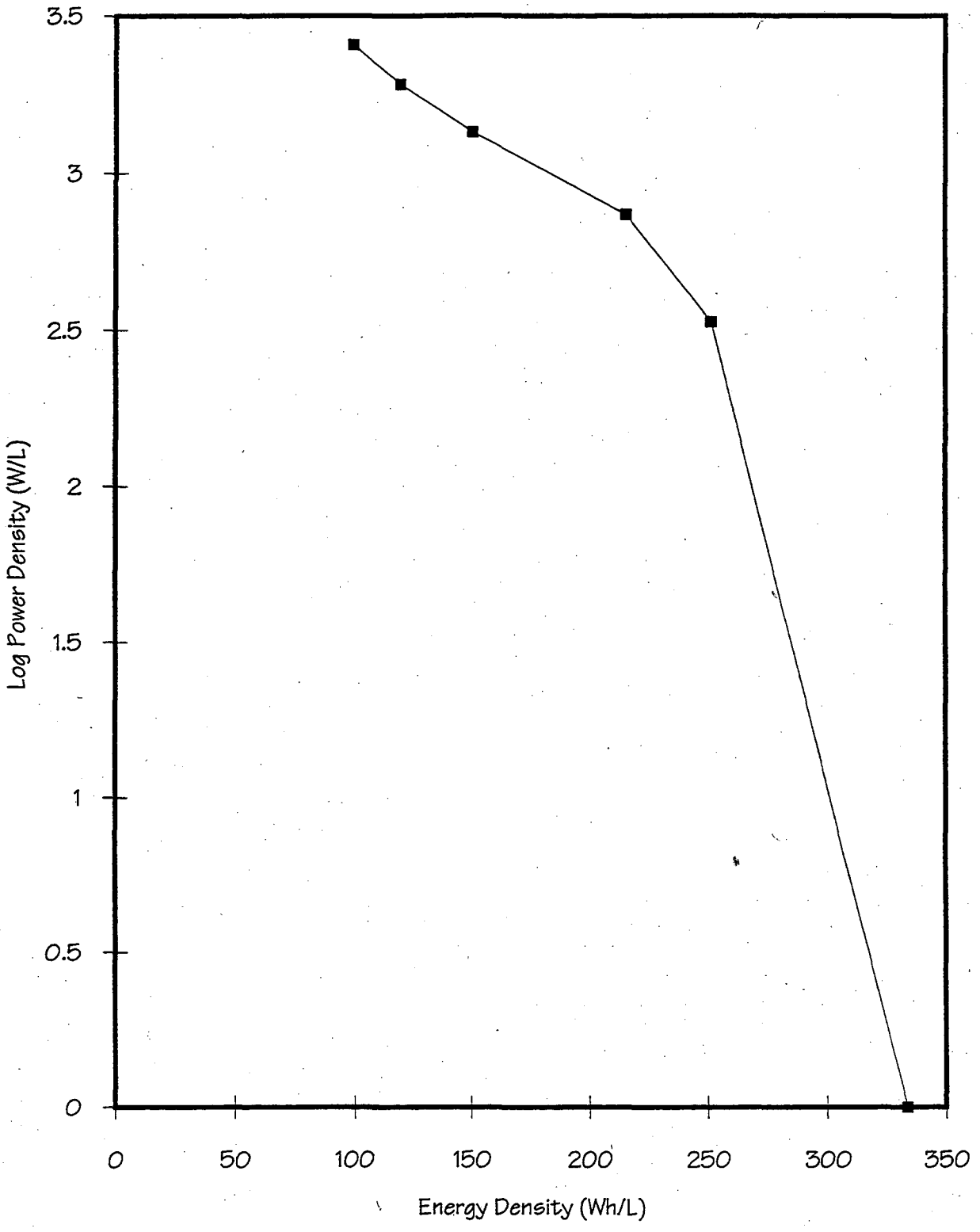
3.5
3
2.5
2
1.5
1
0.5
0
Log Power Density (W/L)
0
50
100
150
200
250
300
350
Energy Density (Wh/L)

Figure 15

LAWRENCE BERKELEY LABORATORY
UNIVERSITY OF CALIFORNIA
TECHNICAL INFORMATION DEPARTMENT
BERKELEY, CALIFORNIA 94720